Acta Crystallographica Section B
Structural Science
ISSN 0108-7681

Twinning and intergrowth of rare earth boride carbides

Oliver Oeckler,[a]* Josef Bauer,[b] Viola Duppel,[a] Hansjürgen Mattausch[a] and Arndt Simon[a]

[a]Max-Planck-Institut für Festkörperforschung, Heisenbergstrasse 1, D-70569 Stuttgart, Germany, and [b]Laboratoire de Chimie du Solide et Inorganique Moléculaire, UMR CNRS 6511, Institut de Chimie de Rennes, Université de Rennes 1, F-35042 Rennes CEDEX, France

Correspondence e-mail: oliver.oeckler@gmx.de

Received 1 February 2001
Accepted 16 November 2001

Twins and intergrown crystals of tetragonal rare earth boride carbides, especially those with the $La_5B_2C_6$ structure type, have been investigated by high-resolution electron microscopy and X-ray diffraction. The structure of the twin interface has been determined. It provides an explanation for coherently intergrown domains of different structure. The Sc_3C_4 structure type is remarkable because it is frequently intergrown with $La_5B_2C_6$-type phases. It provides, for instance, a model for the intergrowth of other types, *e.g.* $Gd_4B_3C_4$ and $Gd_5B_2C_5$. The presence of metal-atom square nets in different orientations in the structures accounts for a number of intergrowth phenomena. The possibilities and limitations of X-ray structure determinations are discussed with respect to actual examples.

1. Introduction

During the past few years, boride carbide phases of rare earth metals (Ln) have received increasing interest due to their various physical and structural properties (Bauer *et al.*, 1998, and references cited therein). Whereas one- or two-dimensionally infinite boron–carbon substructures are found in compounds with low valence electron concentration (Wiitkar *et al.*, 1995), the more electron-rich compounds contain quasimolecular B_xC_y entities and, in some cases, additional carbon species (C atoms or C_2 dumbbells). This class of compound is especially interesting from a theoretical point of view and a large number of band structure calculations have been published (Ansel *et al.*, 1996; Bauer *et al.*, 1998; Jardin *et al.*, 2000). The metal atom substructures of the latter compounds can be described as stacking sequences of planar square nets, which may be distorted to a certain extent. Most of the structures are tetragonal and many others are close to tetragonal. The B_xC_y species are located in the voids of the metal-atom framework. Some of the phases exhibit an extremely large range of homogeneity, as indicated, for instance, by the continuous variation of the *c* lattice parameter of tetragonal $Ce_5B_2C_x$ (x = 5–7) between 11.00 and 12.59 Å (Bidaud, 1998; Oeckler, 2000). Of course, this variation is very important for the electron concentration and/or distribution (*e.g.* the presence of conduction electrons in Ln 5*d* states). Unfortunately, X-ray structure determinations proved to be difficult as the crystals are notoriously twinned or consist of intergrown fragments of different compounds. Coherent twinning and/or intergrowth are much more frequently observed than incoherently intergrown fragments. As comparable domain interfaces obviously occur between several types of phases, it is interesting to know the structure of these interfaces and to explain why the twinning is so characteristic. We investigated this problem by high-resolution electron microscopy

(HRTEM) and X-ray diffraction. Only in exceptional cases can single crystals be obtained. We chose these examples to investigate the possibilities and limitations of X-ray structure determinations for the highly absorbing twinned and intergrown crystals of these compounds.

2. Experimental

Samples of rare earth boride carbides were prepared from the elements. Mixtures of powders with the desired composition were compacted in stainless steel dies and the pellets were arc-melted under purified argon. The alloy buttons were turned over and remelted several times in order to increase their homogeneity. Weight losses were checked to be within 1% of the original mass (1 g). Some samples were wrapped in molybdenum foil or placed in carbon crucibles to avoid contamination, annealed in silica tubes under vacuum at 1273 K for *ca* 10 d and subsequently quenched in water.

Powder samples were characterized by a modified Guinier technique (Simon, 1970; detection with imaging plates, Fuji BAS 5000) or a Stoe Stadi P powder diffractometer using capillaries sealed under dried argon to avoid hydrolysis. Crystals for X-ray investigations were checked for their quality by Laue and precession photographs. Lattice parameters and diffraction data were obtained with a Nonius CAD4 four-circle diffractometer (Ag $K\alpha$ radiation) and a Stoe IPDS one-circle diffractometer with imaging plate area detector (Mo $K\alpha$ radiation). The diffractometer software (Stoe & Cie, 1998) and the *SHELX* suite of programs (Sheldrick, 1997) were used to evaluate the data.

Electron diffraction patterns and high-resolution images were taken with a Philips CM30/ST transmission electron microscope operated at 300 kV using a GATAN slow-scan CCD camera or photographic film. The specimens were prepared by grinding the samples in Ar atmosphere and spreading the powder onto a perforated carbon film supported by a copper grid. The programs *DIFPAT* (Skarnulis *et al.*, 1979) and *EMS* (Stadelmann, 1987) were used for the calculation of (kinematical) diffraction patterns and for image simulations (multislice method), respectively.

3. Twinning of '$La_5B_2C_6$'-type phases

The phases which exhibit the metal-atom arrangement of '$La_5B_2C_6$' (Bauer & Bars, 1982, 1983) are most remarkable owing to their range of homogeneity mentioned above. Recently, the structure of $La_5B_2C_6$ (space group $P4/ncc$) itself has been analysed and described in detail (Oeckler *et al.*, 2001). Essentially, slightly distorted planar square nets of Ln atoms are stacked as shown in Fig. 1. They are displaced against each other and occur in two positions, rotated against each other by 35°. This stacking results in two kinds of large voids which can be filled with interstitial species (Fig. 2). There are chains of octahedral voids along the [001] direction, which are twisted due to the 35° rotation. They are almost empty in the case of $La_5B_2C_6$, but can be partially or completely filled with C atoms or C_2 groups or a mixture of both in other compounds (Oeckler, 2000). Between these chains larger Ln

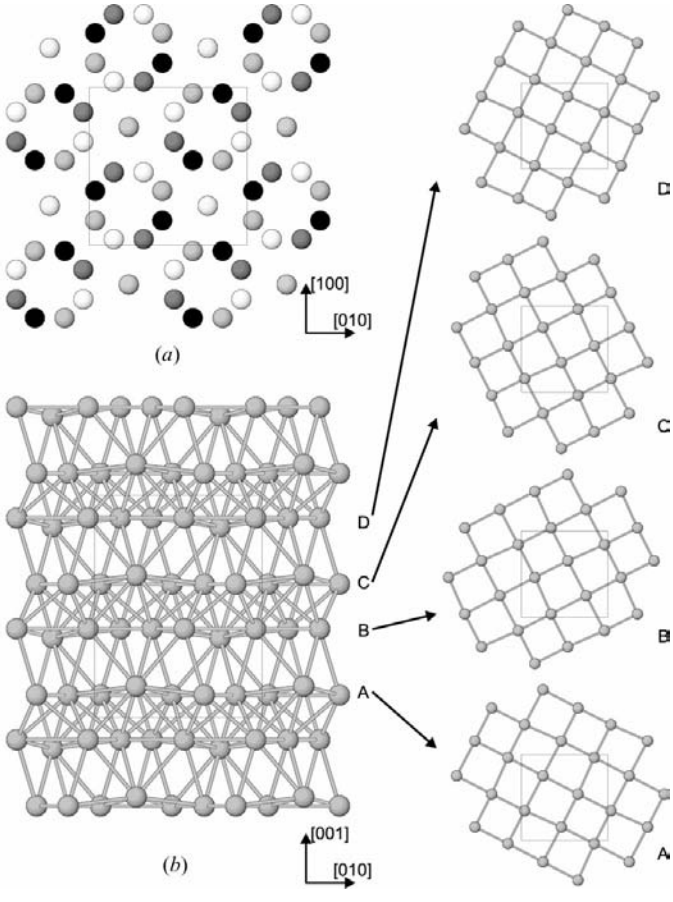

Figure 1
Arrangement of the metal atoms in $La_5B_2C_6$ and related phases: (*a*) projection along [001] (the darker the atoms are shaded, the farther away they are); (*b*) projection along [100], the marked layers are shown individually on the right-hand side in projections along [001]. Lines are drawn between atoms closer than 4 Å.

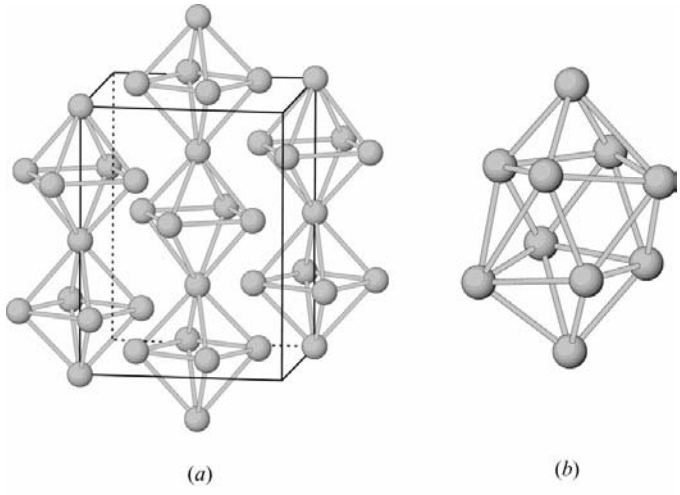

Figure 2
(*a*) Chains of octahedra in the $La_5B_2C_6$ structure type. Only selected interatomic distances are drawn as lines, the origin of the unit cell is shifted to the vertex of one octahedron; (*b*) distorted bicapped tetragonal antiprism of La atoms in $La_5B_2C_6$.

atom polyhedra, namely distorted bicapped tetragonal antiprisms, are formed. They contain zigzag-shaped CBCC entities as in $La_5B_2C_6$ or almost linear CBC groups in the case of the later Ln metals.

Whereas single crystals of most rare earth boride carbides can be obtained by checking a number of crystals, only one out of *ca* 400 crystals of this structure type was found to be a high-quality single crystal for accurate X-ray investigations. The exact composition, *i.e.* the nature of the interstitial species, or the particular Ln element used have no influence whatsoever on the occurrence of twins, but the early Ln elements tend to form larger domains or crystals, respectively. Most crystals are lamina-shaped, with [001] being perpendicular to the platelets according to X-ray measurements. Optical microscopy of polished sections show that most crystals consist of two large twin domains (Fig. 3). The twin boundaries extend in the plane of the lamina and are found approximately in the middle of the crystals. This suggests that the crystals start growing from a very thin lamina at the twin boundary and that the twin boundary $\perp$ [001] consists of a planar metal-atom square net common to both domains. In contrast, the twin law, which can easily be deduced from X-ray diffraction patterns (similar to the electron diffraction diagrams in Fig. 4), is a mirror plane $\perp$ <210> (Bidaud *et al.*, 2000). This has also been found for the related compound Sc_3C_4 (Pöttgen & Jeitschko, 1991; see §4), but in that case it was easy to find untwinned crystals and the twinning was not further investigated.

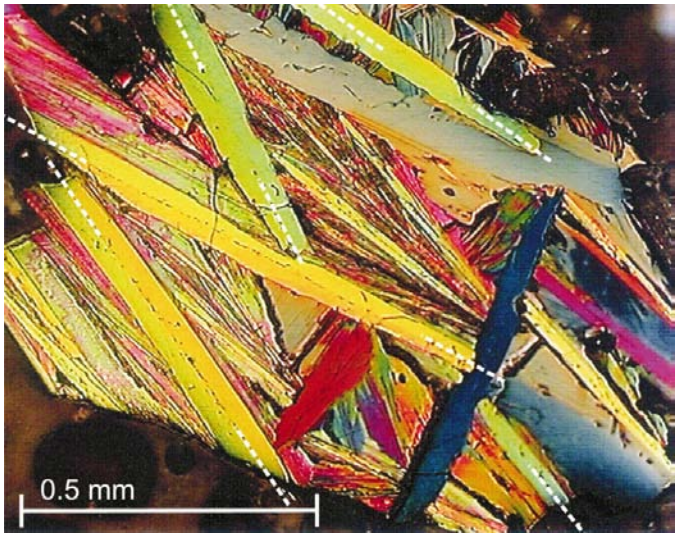

Figure 3
Polished section of $Ho_5B_2C_5$ in polarized light (interference colours are most intensive after slight oxidation of the surface in air), the positions of some twin boundaries are marked by dashed lines.

The insight obtained by X-ray and optical methods is confirmed and can be interpreted by the results of electron diffraction (Fig. 4) and HRTEM (Fig. 5). Selected area diffraction patterns along the [001] zone axis in twinned regions show overlapping patterns of the individual domains and secondary diffraction in nodes of the twin lattice. HRTEM images show a broad zone of overlap and adjoining non-overlapping parts. From these parts diffraction patterns can be obtained which do not exhibit contributions of the other domain. In contrast, sharp twin boundaries are observed in directions perpendicular to [001]. Fig. 5 can be used to determine the relative position of the domains. As HRTEM images can be easily related with structure projections in this

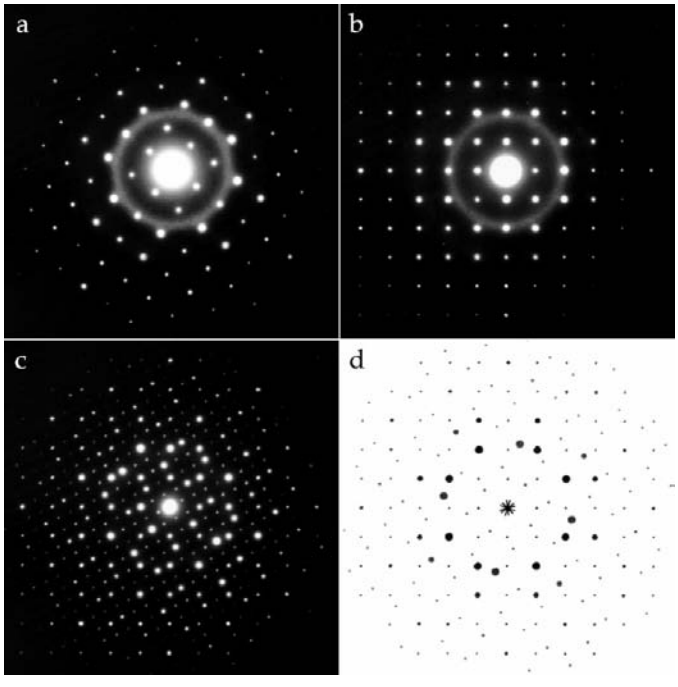

Figure 4
Selected area electron diffraction diagrams of different parts of a $Pr_5B_{\simeq 2}C_{\simeq 6}$ crystallite: (*a*) and (*b*) diagrams from the two separate domains without contribution from the other domain; (*c*) from a part of the crystallite where the two domains overlap with weak reflections due to secondary diffraction; (*d*) superimposed patterns simulated on the basis of X-ray data (kinematical approximation).

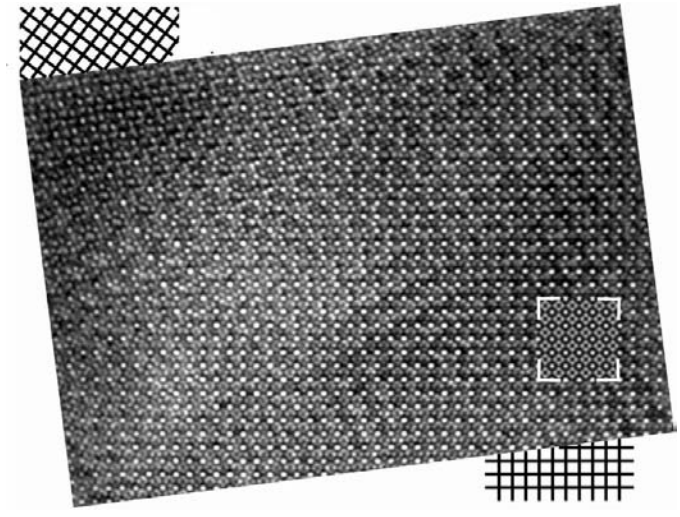

Figure 5
HRTEM image of the crystallite from which the diffraction patterns in Fig. 4 have been taken, zone axis [001]; on two sides of the image the orientations of the domains are emphasized. Between the untwinned parts a broad area of overlap can be seen (inset: image simulation for the untwinned structure based on X-ray data, $t = 3.6$ nm, $\Delta f = -45$ nm).

case of a simple heavy atom arrangement, a structure model for the twin can be derived from the overlapping part of Fig. 5 using a suitable supercell, as shown in Fig. 6. Assuming one common metal-atom layer, a large supercell has been constructed in space group $P4$ by stacking slabs with the thickness of two conventional unit cells along c. An image simulation based on this structure model (not taking B and C into account) fits the observed HRTEM image (Fig. 7) except for some irregular contrast variations, which are not surprising as the domains of the crystallite investigated have no constant thickness and the image quality is reduced by amorphous layers on the surface of the crystallites. The fourfold axes of the domains coincide. One of the two orientations of the planar square nets present in the crystal structure is the same in both twin domains, the other nets are rotated by +35° in one and by −35° in the other domain. The net which has the same orientation in both domains corresponds to the common layer at the twin boundary. Probably the twinning occurs at the very beginning of the crystal growth, when it is not yet dominated by long-range order, and starting from the twin boundary the two differently rotated nets can be arranged on the first slabs. This would also explain why usually a single twin boundary in the middle of the crystal was found.

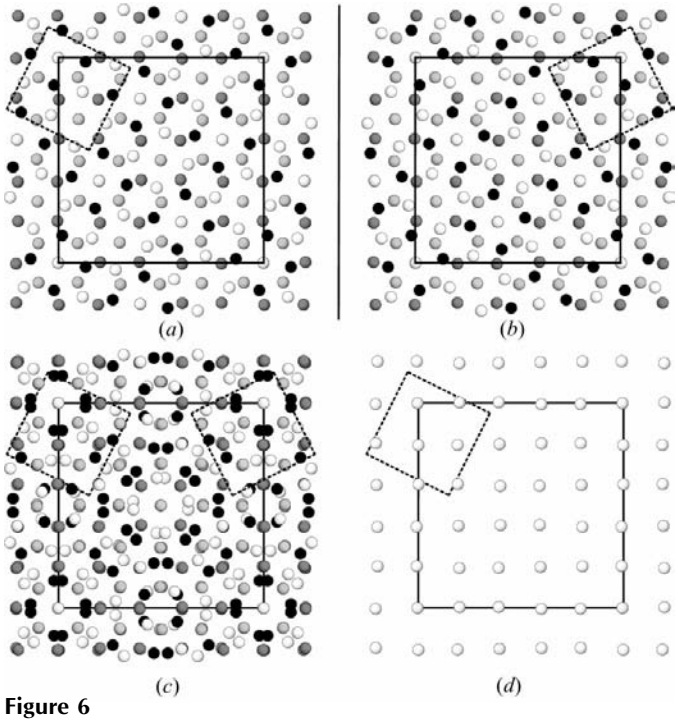

Figure 6
Projections of the structure of $La_5B_2C_6$-type phases. The conventional tetragonal unit cell is drawn with dashed lines, the larger cell (solid lines) allows the use of the same lattice translations for the description of both the structure (*a*) and its mirror image (*b*) with respect to a mirror plane (210). Superposition of (*a*) and (*b*) produces image (*c*) when the edges of the large cells coincide; this view has the highest similarity with the overlapping region in Fig. 5. (*d*) shows one planar square net which has the same position in both orientations.

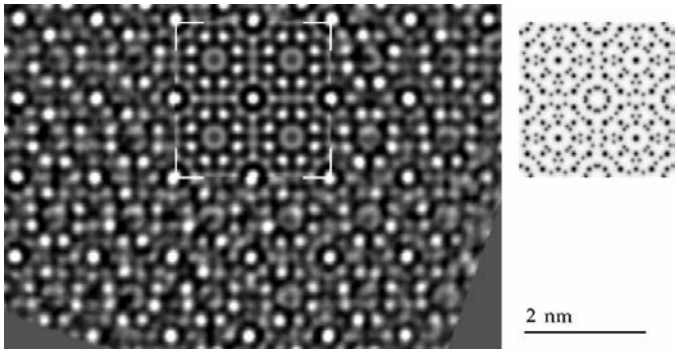

Figure 7
HRTEM image of twinned $Pr_5B_{\simeq 2}C_{\simeq 6}$ (zone axis [001], part of the image shown in Fig. 5) with image simulation (inset, $\Delta f = -50$ nm); on the right the projected potential is shown for comparison (images rotated by 45° with respect to Fig. 6). The image simulation is based on one supercell with 200 heavy atoms in $P4$ with a and b translations as shown in Fig. 6; along c a slab of each twin domain with two unit cells thickness (one common square net) was assumed.

4. Intergrowth of different tetragonal rare earth boride carbides

Especially in the case of the late Ln metals, crystals of the $La_5B_2C_6$ type are frequently intergrown with domains of the Sc_3C_4 type (Pöttgen & Jeitschko, 1991). Sc_3C_4-type phases crystallize in $P4/mnc$ and are closely related to phases such as $La_5B_2C_6$. The C_3 units in Ln_3C_4 can be replaced by CBC groups, resulting in the formula $Ln_{15}B_4C_6$ in the case of a complete replacement. For the same Ln element, a lattice parameters are almost the same and c for the Sc_3C_4 type is *ca* 1.5 times that of the $La_5B_2C_6$ type. Indeed, the Sc_3C_4 type has all the structure elements of $La_5B_2C_6$. In addition Ln–C layers are inserted between the sandwich-like slabs in Sc_3C_4-type phases. The similarity of both types is shown in Fig. 8. The identical parts of the two structure types can constitute interfaces between coherently grown-together domains.

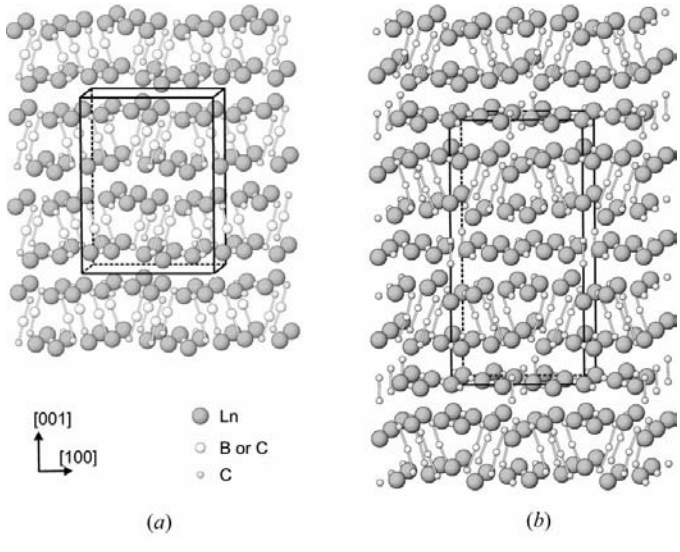

Figure 8
Crystal structures of $Ho_5B_2C_5$ (*a*) and idealized Ho_3C_4 with Sc_3C_4 structure (*b*). The composition of real crystals of the latter type may vary between Ho_3C_4 ($\simeq Ho_{15}C_{20}$) and $Ho_{15}B_4C_{16}$; additional square planar Ho nets with C atoms and C_2 groups are present in that structure.

Domains of both compounds may intergrow either with the corresponding basis vectors of their unit cells axes parallel or rotated against each other in the same way as domains of one compound are fused in twins. Complex X-ray or electron diffraction patterns can easily be explained as superimposed patterns from both compounds with or without additional twinning when projections and sections of reciprocal space are analysed. HRTEM images clearly confirm that the interfaces are $\perp$ [001] and consist of common sandwich-like slabs. Fig. 9 shows an example of a coherent interface between $Ho_5B_2C_5$ and the corresponding compound with Sc_3C_4-type structure.

5. Intergrowth with other rare earth boride carbides

Simultaneous twinning and intergrowth of different phases is also observed with compounds which are not tetragonal, but exhibit comparable square nets of Ln atoms. For example, $Gd_4B_3C_4$ (Jardin *et al.*, 2000) is triclinic, however, the lattice parameters are close to tetragonal. Several complex X-ray diffraction patterns of crystals in the Gd–B–C system can be interpreted assuming four domains. Two of these domains correspond to twinned $Gd_5B_2C_5$ (Bidaud *et al.*, 2000) with the twin plane (210) as mentioned above. The remaining reflections can be indexed assuming two $Gd_4B_3C_4$ domains, related by a mirror plane $\perp$ [100] corresponding to a Ln atom square net. These nets extend in the (100) plane in the latter compound, so they are parallel to the (001) plane, *i.e.* the square nets, of the two $Gd_5B_2C_5$ individuals. Again one can assume that the domain interfaces are exactly these square nets, but HRTEM investigations do not seem feasible due to the triclinic symmetry (with tetragonal pseudo-symmetry) of $Gd_4B_3C_4$. However, Fig. 10 shows that the structure of Sc_3C_4-like phases may provide a model for the intergrowth of $Gd_4B_3C_4$ (which has only exactly planar Gd nets) with $Gd_5B_2C_5$, where the nets are somewhat corrugated. In the Sc_3C_4 type both exactly planar and corrugated layers are stacked upon each other.

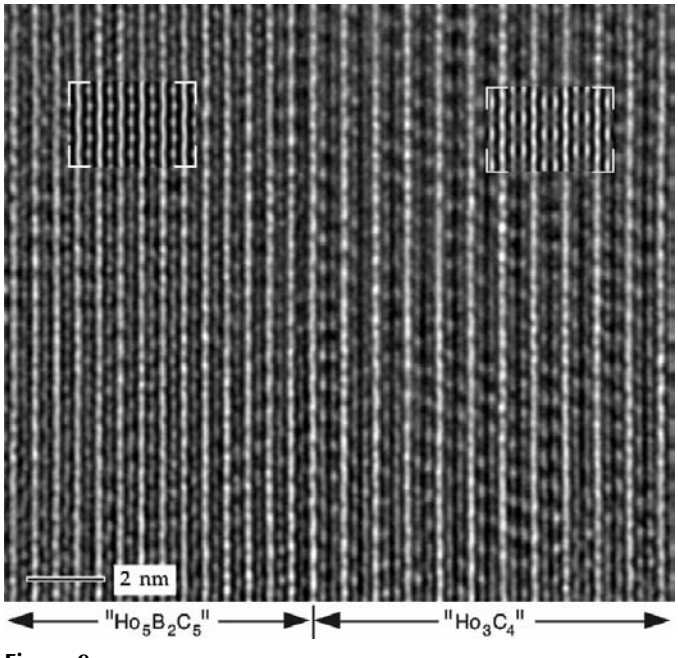

Figure 9
HRTEM image of intergrown domains of '$Ho_5B_2C_5$' and 'Ho_3C_4' (*cf.* text), zone axis [100], with image simulations (insets) for the two domains (t = 3.2 nm, Δf = −35/−40 nm), showing a sharp domain boundary.

6. X-ray structure analysis of twinned and intergrown crystals

Single crystals for accurate X-ray structure determinations could be obtained for at least one example of all the above-mentioned structure types. Twinned and intergrown crystals must be used for the analysis of a large number of solid solution members in order to elucidate the nature of the range of homogeneity (which is due to different possibilities of filling the voids of the Ln substructure with different B–C species). Therefore, it is interesting to compare the results for single and twinned or intergrown crystals of the same compound. With rare earth compounds, absorption effects rather than counting statistics are the bottleneck for data accuracy, so it is highly advisable to select very small crystals. No really satisfactory absorption corrections are known for twinned and intergrown crystals, and existing analytical corrections are not applicable. It is by far the best compromise to measure datasets with high redundancy and to apply Blessing's (1995) multi-scan correction. In the case of lamina-shaped crystals where layers of the different domains are grown upon each other, single-crystal absorption corrections are a good approximation, as shading effects are about the same for all reflections (of one domain) if one avoids diffraction planes perpendicular to the platelet. This means that the primary beam should not lie within the plane in which the lamina extends. In the examples mentioned above, this kind of layered lamina-shaped crystal is fairly common, so that the

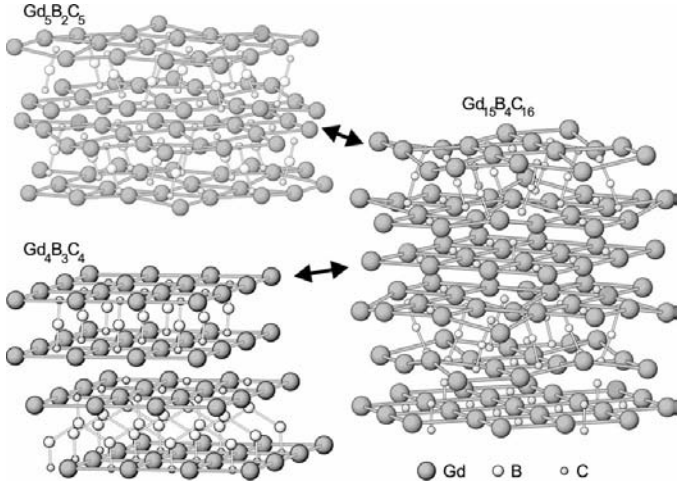

Figure 10
Representations of the structures of $Gd_4B_3C_4$ and $Gd_5B_2C_5$ compared with hypothetical $Gd_{15}B_4C_{16}$ derived from the Sc_3C_4 type by replacing C_3 units by CBC groups. The lines between the Ln atoms emphasize the layer-like arrangement of Ln atom square nets, but do not show all short Ln—Ln distances.

Table 1
Comparison of refinement results for a single and a twinned crystal of $La_5B_2C_6$ (Stoe IPDS diffractometer, Mo$K\alpha$ radiation; room temperature; numerical absorption correction for the single crystal, multi-scan correction for the twinned crystal).

An accurate single-crystal structure determination has already been published (Oeckler *et al.*, 2001; refer to this article for details such as atom numbering *etc.*).

		Single crystal	Twin *all data*	Twin domain 1	Twin domain 2
Lattice parameters (Å)		a = 8.590 (1) c = 12.398 (1) (powder data)		a = 8.574 (5) c = 12.370 (8)	
R_{int} (4/m), R_σ		0.043, 0.013	–, 0.011	0.067, 0.009	0.071, 0.009
R_1, wR_2 [$I > 2\sigma(I)$]		0.020, 0.052	0.058, 0.161	0.059, 0.174	0.062, 0.176
R_1, wR_2 (all data)		0.043, 0.060	0.082, 0.185	0.078, 0.198	0.080, 0.199
GOF		1.044	1.064	1.122	1.112
$\Delta\rho_{max}$, $\Delta\rho_{min}$ (e Å^{-3})		+1.88, −1.13	+5.18, −2.78	+4.19, −2.38	+5.60, −3.04
La1	x	0.65003 (6)	0.65047 (5)	0.65059 (7)	0.65034 (7)
	y	0.05107 (6)	0.05017 (5)	0.05007 (7)	0.05029 (8)
	z	0.10729 (3)	0.10729 (3)	0.10730 (4)	0.10726 (4)
	u_{11}	0.0073 (2)	0.0082 (3)	0.0078 (4)	0.0082 (4)
	u_{22}	0.0102 (2)	0.0121 (3)	0.0116 (4)	0.0120 (4)
	u_{33}	0.0271 (2)	0.0269 (3)	0.0277 (4)	0.0277 (4)
	u_{ij} ($i \neq j$)	< 0.001	< 0.002	< 0.002	< 0.002
La2	z	0.13679 (6)	0.13619 (9)	0.13588 (13)	0.13598 (13)
	$u_{11} = u_{22}$	0.0080 (3)	0.0078 (3)	0.0073 (4)	0.0080 (4)
	u_{33}	0.0401 (4)	0.0525 (6)	0.0553 (9)	0.0509 (9)
C1—C2/B2	1.34 (2)	1.34 (2)	1.36 (3)	1.34 (3)	
C2/B2—C2/B2	1.53 (3)	1.46 (2)	1.44 (3)	1.48 (3)	
La2—C1	2.72 (1)	2.72 (1)	2.75 (2)	2.68 (2)	
La2—C2/B2	2.96 (1)	3.00 (1)	3.01 (1)	2.99 (2)	
La1—C3	2.78 (3)	2.75 (2)	2.76 (2)	2.73 (4)	
C1—C2/B2—C2/B2	156 (1)	159 (1)	159 (2)	161 (2)	

Table 2
Comparison of structure determinations of $Gd_4B_3C_4$.

Single-crystal data from Jardin *et al.* (2000) and data (same method and parameters for the data collection) from a twin intergrown with $Gd_5B_2C_5$ as described in the text.

	Single crystal	Twin domain 1	Twin domain 2
Lattice parameters (Å, °)†	a = 3.637 (2) b = 3.674 (2) c = 11.850 (5) α = 93.34 (5) β = 96.77 (5) γ = 90.24 (5)	a = 3.625 (4) b = 3.656 (2) c = 11.91 (1) α = 92.6 (1) β = 97.0 (1) γ = 90.1 (1)	a = 3.625 (4) b = 3.655 (2) c = 11.92 (1) α = 92.5 (1) β = 97.2 (1) γ = 90.2 (1)
Unique data/parameters	740/33	467/31	471/31
R_{int}, R_σ	0.038, 0.043	0.123, 0.023	0.143, 0.027
R_1, wR_2 [$I > 2\sigma(I)$]	0.040, 0.107	0.081, 0.180	0.096, 0.219
R_1, wR_2, GOF (all data)	0.053, 0.111, 1.16	0.085, 0.183, 1.37	0.100, 0.231, 1.44
$\Delta\rho_{max}$, $\Delta\rho_{min}$ (e Å^{-3})	+5.6, −2.4	+4.1, – 4.5	+4.9, −5.0
E.s.d. of Gd—Gd distances (Å)	≤ 0.002	≤ 0.004	≤ 0.005
Shortest Gd—Gd distance (Å)	3.322 (2)	3.295 (4)	3.295 (5)
CBC unit: B—C distance (Å)	1.48 (2)	1.48 (4)	1.51 (4)
$(BC)_\infty$ chain: B—C distance (Å)	1.45 (5)	1.44 (5)	1.40 (6)
B—B distances (Å)	2.06 (9)/2.18 (9)	1.78 (9)/2.42 (9)	1.8 (1)/2.4 (1)

results of structure determinations are surprisingly reliable. Only a few representative examples are given here.

In the case of $La_5B_2C_6$-type phases, where twinning by reticular merohedry is present, it is necessary to include reflections common to both domains in refinements, as a high percentage of the crystal's total reflected intensity concentrates in these overlapping reflections. In contrast, it is normally not necessary to include non-overlapping reflections of both domains (Herbst-Irmer & Sheldrick, 1998). In intergrown crystals or those with lower symmetry, the data quality is inferior because partially overlapping reflections of different domains have to be excluded.

The structure determination of $La_5B_2C_6$ (Oeckler *et al.*, 2001) has shown that anharmonic displacement parameters are necessary for the optimal fit of single-crystal data. Anharmonic refinements proved to be inadequate in the case of twins, as the resulting probability density function is physically impossible. For this reason, usual anisotropic refinements are compared in Table 1. In that case, the inclusion of all reflections yields slightly better results than using data from only one domain because the domains were approximately of equal size. Due to obvious systematic errors, the parameters for single and twinned crystals differ somewhat more than their e.s.d.'s indicate. However, although R values and residual densities are higher for the twin, even boron and carbon positions can easily be refined, and interatomic distances do not differ significantly if a 3σ reliability interval is taken into account.

For intergrown crystals of the tetragonal compounds mentioned in §4 the reliability of the results is comparable to that of the results for $La_5B_2C_6$. In many cases all light atom positions could be easily located from difference Fourier maps and refined, but simultaneous refinement of their occupancy and temperature factors is only possible with single-crystal data. Even if some datasets are rather incomplete due to partially overlapping reflections and some refinements might not be acceptable for the standard determination of a novel structure, the refinements are very valuable in order to confirm the interpretation of complex diffraction patterns. In the most unfavourable cases the light atom positions may have little precision, but they become much less ambiguous if their environment is taken into account. The results can be important in order to reveal new structure types and to obtain the proper composition for new synthetic approaches in the complicated Ln–B–C systems.

Table 2 shows results obtained for a twinned $Gd_4B_3C_4$ crystal which is intergrown with twinned $Gd_5B_2C_5$ (as described in §5) compared with the single-crystal result. Even in this unfavourable case the agreement is obvious. The results for the $Gd_5B_2C_5$ part are equally consistent with Bidaud *et al.*'s (2000) single-crystal data.

7. Conclusions

Rare earth boride carbides with tetragonal or pseudo-tetragonal metal-atom arrangements exhibit a pronounced tendency to form twins and coherently intergrown domains of different phases. We have shown that this tendency is due to structure elements common to all phases. These elements are (nearly) planar square nets of Ln atoms or even sandwich-like slabs, which are present in different orientations and constitute the interfaces between different domains. Reasonable structure refinements on X-ray data can be obtained from twinned and/or intergrown crystals, but some fine details of the structures can only be revealed from single-crystal data.

We thank Roland Eger for preliminary X-ray investigations on a large number of crystals.

References

Ansel, D., Bauer, J., Bonhomme, F., Boucekkine, G., Frapper, G., Gougeon, P., Halet, J.-F., Saillard, J.-Y. & Zouchoune, B. (1996). *Angew. Chem.* **108**, 2245–2248.
Bauer, J. & Bars, O. (1982). *J. Less-Common Met.* **83**, 17–27.
Bauer, J. & Bars, O. (1983). *J. Less-Common Met.* **95**, 267–274.
Bauer, J., Halet, J.-F. & Saillard, J.-Y. (1998). *Coord. Chem. Rev.* **178–180**, 723–753.
Bidaud, E. (1998). PhD thesis. Université de Rennes 1, France.
Bidaud, E., Hiebl, K., Hoffmann, R.-D., Pöttgen, R., Jardin, C., Bauer, J., Gautier, R., Gougeon, P., Saillard, J.-Y. & Halet, J.-F. (2000). *J. Solid State Chem.* **154**, 286–295.
Blessing, R. H. (1995). *Acta Cryst.* A**51**, 33–38.
Herbst-Irmer, R. & Sheldrick, G. M. (1998). *Acta Cryst.* B**54**, 443–449.
Jardin, C., Oeckler, O., Mattausch, Hj., Simon, A., Halet, J.-F., Saillard, J.-Y. & Bauer, J. (2000). *Inorg. Chem.* **39**, 5895–5900.
Oeckler, O. (2000). PhD thesis. Universität Stuttgart, Germany.
Oeckler, O., Bauer, J., Mattausch, Hj. & Simon, A. (2001). *Z. Anorg. Allg. Chem.* **627**, 779–788.
Pöttgen, R. & Jeitschko, W. (1991). *Inorg. Chem.* **30**, 427–431.
Sheldrick, G. M. (1997). *SHELX*97. University of Göttingen, Germany.
Simon, A. (1970). *J. Appl. Cryst.* **3**, 11–18.
Skarnulis, A. J., Liljestrand, G. & Kihlborg, L. (1979). *Chem. Commun.* **1**, 1–27.
Stadelmann, P. (1987). *Ultramicroscopy*, **21**, 131–146.
Stoe & Cie (1998). *Stoe IPDS Software Package*, Version 2.89. Darmstadt, Germany.
Wiitkar, F., Kahlal, S., Halet, J.-F., Saillard, J.-Y., Bauer, J. & Rogl, P. (1995). *Inorg. Chem.* **34**, 1248–1256.